

# Coherence in Microchip Traps

Philipp Treutlein,\* Peter Hommelhoff,<sup>†</sup> Tilo Steinmetz, Theodor W. Hänsch, and Jakob Reichel  
*Max-Planck-Institut für Quantenoptik und Sektion Physik der  
 Ludwig-Maximilians-Universität, Schellingstr.4, 80799 München, Germany*  
 (Dated: February 9, 2020)

We report the coherent manipulation of internal states of neutral atoms in a magnetic microchip trap. Coherence lifetimes exceeding 1 s are observed with atoms at distances of  $4 - 130 \mu\text{m}$  from the microchip surface. The coherence lifetime in the microtrap is independent of atom-surface distance and agrees well with the results of similar measurements in macroscopic magnetic traps. Due to the absence of surface-induced decoherence, a miniaturized atomic clock with a relative stability in the  $10^{-13}$  range can be realized. For applications in quantum information processing, we propose to use microwave near-fields in the proximity of chip wires to create potentials that depend on the internal state of the atoms.

Magnetic microchip traps provide one of the few available techniques for the manipulation of neutral atoms on the micrometer scale, and the only technique so far that enables nonperiodic, built-to-purpose micron-sized potentials [1]. The on-chip creation of Bose-Einstein condensates [2, 3] and the highly controlled manipulation of atomic motion in ‘atomic conveyor belts’, waveguides, and thermal beam splitters [1] are examples of the versatility of such ‘atom chips’. Due to these experimental possibilities, atoms in microtraps are promising candidates for the implementation of quantum gates [4], quantum simulations [5], and interferometric sensors [6]. The ability to create and manipulate superpositions of internal states of the trapped atoms is essential for most of these applications. In the context of quantum information processing (QIP), two internal states  $|0\rangle$  and  $|1\rangle$  of the atom serve as qubit states. To perform quantum gate operations, long coherence lifetimes of the superposition states  $\alpha|0\rangle + \beta|1\rangle$  are required and therefore decoherence processes have to be avoided. Atoms in magnetic microtraps, however, can potentially suffer from a reduction of the coherence lifetime due to interaction with the surface of the microchip [7], in addition to other decoherence mechanisms which are also present in macroscopic traps [8].

In this paper, we demonstrate coherent manipulation of internal atomic states in a magnetic microtrap. We create superpositions of two hyperfine ground states of  $^{87}\text{Rb}$  atoms in a thermal ensemble close to quantum degeneracy and perform Ramsey spectroscopy to determine the coherence lifetime (Fig. 1). With atoms at distances of  $4 - 130 \mu\text{m}$  from the surface of the chip, we observe coherence lifetimes exceeding 1 s. The measured coherence lifetimes are independent of the atom-surface distance, and agree well with those observed in macroscopic magnetic traps [8].

The observed robustness of the superposition states is an extremely encouraging result for atom chip applications in QIP and opens a new perspective on applications in precision metrology. We demonstrate an atomic clock in the microtrap and measure the relative stability of

its transition frequency. Our measurements show that a portable atom chip clock with a relative stability in the  $10^{-13}\tau^{-1/2}/\sqrt{\text{Hz}}$  range is a realistic goal.

To realize the collisional phase gate proposed in [4], a method to create state-selective potentials is needed. We point out that internal state selectivity for our state pair can be provided by microwave trapping potentials. These potentials, considered in the early 90s [9, 10] but abandoned later, gain new actuality as near-field traps on atom chips.

To achieve long coherence lifetimes with magnetically trapped atoms, we choose the  $|F = 1, m_F = -1\rangle \equiv |0\rangle$  and  $|F = 2, m_F = 1\rangle \equiv |1\rangle$  hyperfine levels of the  $5S_{1/2}$  ground state of  $^{87}\text{Rb}$ . The magnetic moments and the corresponding Zeeman shifts of the two states are approximately equal. This greatly reduces spatial inhomogeneities of the transition frequency  $\nu_{10}$  in the magnetic trap, since both states experience approximately the same trapping potential. Furthermore, superpositions of this state pair are particularly robust against decoherence due to temporal magnetic field fluctuations. At a magnetic field of  $B_0 \sim 3.23 \text{ G}$ , both states experience the same first-order Zeeman shift and the magnetic field dependence of  $\nu_{10}$  is minimized [8]. In all of our experiments, we therefore adjust the field in the center of the trap to  $B_0$ .

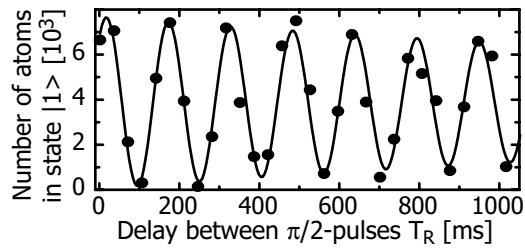


FIG. 1: Ramsey spectroscopy of the  $|0\rangle \leftrightarrow |1\rangle$  transition with atoms held at a distance  $d = 8 \mu\text{m}$  from the chip surface. An exponentially damped sine fit to the Ramsey fringes yields a  $1/e$  coherence lifetime of  $\tau_c = 2.8 \pm 1.6 \text{ s}$ . Each data point corresponds to a single shot of the experiment.

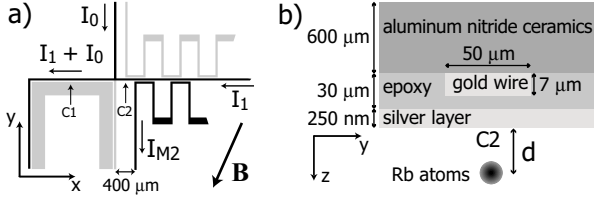


FIG. 2: (a) Layout of the relevant wires on the chip substrate.  $C_1$  indicates the position of the initial magnetic trap. The ‘measurement trap’ used in the experiments is located at position  $C_2$ . (b) Layer structure of the microtrap substrate and atom-surface distance  $d$  of the measurement trap at position  $C_2$ . Current is carried by gold wires  $\sim 30 \mu\text{m}$  below the chip surface.

Our experimental setup has been previously described [3, 11]. The magnetic micropotentials are created by sending currents through microscopic gold conductor patterns on an aluminum nitride substrate and superposing a homogeneous, external bias field (Fig. 2). The preparation of the atomic ensemble proceeds in a multi-step sequence involving loading of the microtrap from a mirror-MOT, compression of the trap and evaporative cooling [3]. By the end of this sequence, a Ioffe-type ‘measurement trap’ which is centered at the position  $C_2$  in Fig. 2a contains a thermal atomic ensemble of typically  $1.5 \times 10^4$  atoms in state  $|0\rangle$  at a temperature of 600 nK. The measurement trap is created by the wire currents  $I_0$ ,  $I_1$ , and  $I_{M2}$  and the bias field  $\mathbf{B} = (B_x, B_y, 0)$  shown in Fig. 2a. By adjusting all three currents and  $B_y$ , the atoms can be placed at distances  $d = 0 - 130 \mu\text{m}$  from the chip surface (see Fig. 2b) without relevant changes in the shape of the magnetic potential. For each experimentally studied distance, the field  $\mathbf{B}_{\min}$  at the center of the trap was calibrated spectroscopically [8] and set to  $|\mathbf{B}_{\min}| = B_0$  by adjusting  $B_x$ . Typical experimental parameters are  $I_0 = 500 \text{ mA}$ ,  $I_1 = 120 \text{ mA}$ ,  $I_{M2} = 700 \text{ mA}$ ,  $B_y = -5.50 \text{ G}$ , and  $B_x = -2.18 \text{ G}$ , leading to trap frequencies  $(f_x, f_y, f_z) = (50, 350, 410) \text{ Hz}$  at  $d = 8 \mu\text{m}$ . The atoms are held in the measurement trap while the coherent internal state manipulation is performed. After the manipulation, the trap is switched off within 150  $\mu\text{s}$  and the atoms are detected after a time-of-flight of typically 4 ms. Atoms are detected by absorption imaging on the  $F = 2 \rightarrow F' = 3$  transition. This allows direct determination of the number of atoms in state  $|1\rangle$ ,  $N_1$ . To alternatively determine the number of atoms in state  $|0\rangle$ ,  $N_0$ , we first blow away all atoms in  $|1\rangle$  with the resonant probe light. The  $|0\rangle$  atoms are then optically pumped to  $|F = 2, m_F = +2\rangle$  and imaged as before.

Coherent internal state manipulation is achieved by coupling the states  $|0\rangle$  and  $|1\rangle$  through a two-photon microwave-rf transition. The microwave frequency  $\nu_{\text{mw}}$  is detuned 1.2 MHz above the  $|F = 2, m_F = 0\rangle$  intermediate state and radiated from a sawed-off waveguide outside the vacuum chamber. The radio frequency  $\nu_{\text{rf}}$  is either

applied to the same external coil that is used for evaporative cooling, or to a wire on the chip.  $\nu_{\text{mw}}$  and  $\nu_{\text{rf}}$  are phase locked to a 10 MHz reference from an ultrastable quartz oscillator (Oscilloquartz OCXO 8607-BM, relative stability  $10^{-13}$  from 1 – 30 s, cf. fig. 4). By applying the two-photon drive for a variable time and detecting the number of atoms transferred from  $|0\rangle$  to  $|1\rangle$ , we observe Rabi oscillations with a resonant two-photon Rabi frequency of  $\sim 0.5 \text{ kHz}$ . In this way, single-qubit rotations can be realized. The maximum transition probability, corresponding to a  $\pi$ -pulse, is  $N_1/(N_0 + N_1) = 95 \pm 5 \%$ .

To test for decoherence of the superposition states, we perform Ramsey spectroscopy [12] by applying the following pulse sequence: The atoms in state  $|0\rangle$  are held in the measurement trap for a time  $T_H$  before a first  $\pi/2$ -pulse creates a coherent superposition of  $|0\rangle$  and  $|1\rangle$ . After a time delay  $T_R$ , a second  $\pi/2$ -pulse is applied, and the resulting state is probed by the detection sequence. Ramsey fringes are recorded in the time domain by varying  $T_R$  while keeping  $\Delta_R = \nu_{\text{mw}} + \nu_{\text{rf}} - \nu_{10}$  fixed ( $\Delta_R \ll \nu_{10} \simeq 6.8 \text{ GHz}$ ). Alternatively, Ramsey fringes are recorded in the frequency domain by scanning  $\Delta_R$  while  $T_R$  remains constant. Loss of coherence of the superposition states can show up in different ways in the Ramsey signal. A spatial variation of  $\nu_{10}$  across the atomic ensemble leads to a decay of the contrast of the Ramsey fringes, while temporal fluctuations of  $\nu_{10}$  lead to increasing phase noise on the Ramsey oscillation as  $T_R$  is increased.

Figure 1 shows Ramsey interference in the time domain. The number of atoms detected in state  $|1\rangle$  oscillates at the frequency difference  $\Delta_R = 6.4 \text{ Hz}$ , while the interference contrast decays with a coherence lifetime of  $\tau_c = 2.8 \pm 1.6 \text{ s}$ . The measurement shown in Fig. 1 was performed at  $d = 8 \mu\text{m}$  from the room-temperature chip surface. In [8], similar coherence lifetimes are reported for the same state pair, but with atoms in a macroscopic magnetic trap, far away from any material objects. This suggests that atom-surface interactions do not limit the coherence lifetime in our present experiment.

To further probe for surface effects, we study the decoherence of the Ramsey signal as a function of atom-surface distance. Atomic ensembles are prepared in measurement traps at different distances  $d$  from the surface. In each trap, we record Ramsey oscillations in the frequency domain for several values of  $T_R$  and determine the contrast  $C(T_R)$  of each oscillation. Figure 3 shows the result of this measurement for  $T_R = 50 \text{ ms}$  and  $T_R = 1 \text{ s}$ . Within the experimental error, the contrast does not show a dependence on atom-surface distance for  $d = 4 - 130 \mu\text{m}$ . In addition, we have compared the signal-to-noise ratio  $S/N$  of the interference signal in the different traps. We typically observe  $S/N = 6$  for  $T_R = 1 \text{ s}$ , where  $S$  is the peak-to-peak amplitude of the sinusoidal fit to the Ramsey oscillation and  $N$  is the standard deviation of the fit residuals over one oscilla-

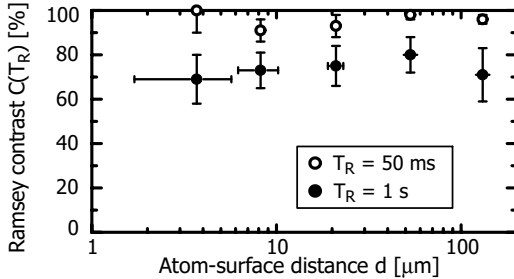


FIG. 3: Contrast  $C(T_R)$  of the Ramsey fringes as a function of atom-surface distance  $d$  for two values of the time delay  $T_R$  between the  $\pi/2$ -pulses. For each data point,  $C(T_R) = (N_{\max} - N_{\min})/(N_{\max} + N_{\min})$  was obtained from a sinusoidal fit to frequency-domain Ramsey fringes.  $N_{\max}$  ( $N_{\min}$ ) is the maximum (minimum) of the oscillation in  $N_1$ .

tion period.  $S/N$  is independent of  $d$ , indicating that the processes causing amplitude and phase fluctuations of the interference signal do not depend on atom-surface distance on this time scale.

The observed decoherence is mainly due to a combination of the residual differential Zeeman shift and the density dependent collisional shift of  $\nu_{10}$  across the ensemble [8]. Consequently, we observe a dependence of the coherence lifetime on the temperature  $T$  and on the peak density  $n_0$  of the ensemble. To avoid systematic errors, we have checked that there is no systematic variation of  $T$  and  $n_0$  in the measurement trap as  $d$  is varied in the range of  $4 - 130 \mu\text{m}$ . For all data points in Fig. 3,  $n_0 < 5 \times 10^{12} \text{ cm}^{-3}$  and  $T < 700 \text{ nK}$ . The observed noise on the Ramsey oscillation is mostly phase noise and can be attributed to ambient magnetic field fluctuations (see below). For  $T_R > 1 \text{ s}$  the phase noise increases and obscures the Ramsey oscillation even before the contrast has completely disappeared.

To calibrate the atom-surface distance  $d$ , which is not identical to the distance of the atoms from the current-carrying wires that create the trapping potential (see Fig. 2b), we use two methods: For  $d > 10 \mu\text{m}$ , we use a technique described in [13] in which the imaging beam is slightly tilted towards the chip surface. A second image reflected by the surface appears and both the surface position and the atom-surface distance can be determined from the vertical positions of the two images. For  $d < 10 \mu\text{m}$ , the distance can no longer be resolved by our imaging system. However, we are able to locate the surface by increasing the bias field  $B_y$  and thereby moving the trap closer to the surface until the atoms are lost in the attractive surface potential. This technique is similar to the measurement of the surface potential in [16]. Once we know the position of the surface and the corresponding value  $B_y^{d=0}$ , the distance  $d$  for  $B_y < B_y^{d=0}$  is inferred from a simulation of the trapping potential. We estimate an uncertainty in the determination of the surface position of  $\pm 2 \mu\text{m}$ , which is included in the error

bars of Fig. 3.

Thermal magnetic field fluctuations driving spin-flip transitions to untrapped states have been predicted [7] and observed [14, 15, 16] to limit the lifetime  $\tau_N$  of the atomic *population* near a surface. We also observe this effect in our experiment. The trap lifetime of atoms in state  $|0\rangle$  decreases from  $\tau_N = 10 \text{ s}$  for  $d > 20 \mu\text{m}$  to  $\tau_N = 1.6 \text{ s}$  for  $d = 4 \mu\text{m}$  (lifetimes for state  $|1\rangle$  are slightly lower). To distinguish this loss of population from the loss of *coherence*,  $T_H + T_R$  is kept constant during the Ramsey scan by appropriately adjusting the hold time  $T_H$  for each value of  $T_R$ . In this way, the overall time the atoms spend close to the surface is independent of  $T_R$ .  $N_0 + N_1$  at the time of detection therefore remains approximately constant (neglecting the lifetime difference) and the loss of atoms does not show up in the Ramsey measurements. However, the atom loss limits the range of distances at which coherence measurements with  $T_R \sim 1 \text{ s}$  can be made to  $d \geq 4 \mu\text{m}$ .

One motivation for microtrap research is the perspective of creating miniaturized cold-atom devices. Due to the long coherence lifetime, it is natural to consider utilizing the  $|0\rangle \leftrightarrow |1\rangle$  transition in an atomic clock on the microchip. We demonstrate the principle of such a clock and measure its frequency stability relative to the quartz reference oscillator. Figure 4b shows frequency-domain Ramsey fringes for an interrogation time of  $T_R = 1 \text{ s}$ . We set the two-photon drive to the slope of the Ramsey resonance, as indicated by the arrow in the figure, and repeat the experiment many times with a cycle period of 23 s. Any temporal drift  $\delta\nu$  of  $\nu_{10}$  with respect to the reference will change  $\Delta_R$  and therefore show up as a variation  $\delta N$  of  $N_1$ . From repeated measurements of  $\delta N$  we determine the relative frequency fluctuations  $\delta\nu/\nu_{10}$ . In Fig. 4a we plot the Allan standard deviation  $\sigma(\tau)$  [18] of  $\delta\nu/\nu_{10}$  as a function of averaging time  $\tau$ . For short averaging times, the Allan standard deviation decreases as  $\sigma(\tau) = 1.7 \times 10^{-11} \tau^{-1/2} / \sqrt{\text{Hz}}$ , corresponding to shot-to-shot fluctuations of  $\delta\nu = 24 \text{ mHz}$  r.m.s. For  $\tau > 6 \times 10^2 \text{ s}$ , the long term drift of the quartz reference leads to a departure from the  $\tau^{-1/2}$  line. We have modeled the frequency fluctuations in our experiment and can account for the observed value of  $\delta\nu$ . It is dominated by ambient magnetic field fluctuations of  $\sim 5 \text{ mG}$  present in our laboratory. Smaller contributions are due to variations of  $\sim 4\%$  in total atom number leading to variations of the density-dependent collisional shift [8], and due to imperfections of the detection system. We estimate that straightforward improvements—magnetic shielding, operation in a shallower trap at lower atomic density, and improved detection—will lead to a frequency stability in the  $10^{-13} \tau^{-1/2} / \sqrt{\text{Hz}}$  range. While this does not reach the stability level of atomic fountain clocks, a chip-based clock has the advantage of a simple, compact and portable design.

Applications of magnetic microtraps in QIP require long coherence lifetimes of the qubit in the presence of un-

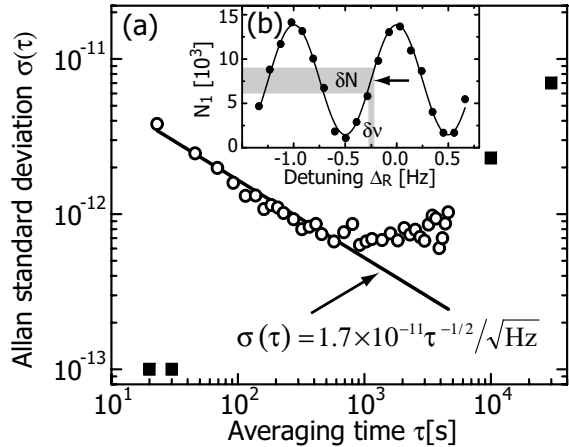


FIG. 4: (a) Measured Allan standard deviation  $\sigma(\tau)$  of the atomic clock in the microtrap compared to the quartz reference oscillator (open circles). The solid line is a fit with  $\sigma(\tau) \propto \tau^{-1/2}$  representing the performance of the atomic clock. For  $\tau > 6 \times 10^2$  s the drift of the quartz reference becomes apparent. The manufacturers' specification of the quartz stability is shown in solid squares. (b) Ramsey resonance for  $T_R = 1$  s in the microtrap at  $d = 53 \mu\text{m}$  from the surface (solid circles). The line is a sinusoidal fit to the data. The arrow indicates the operating point on the slope of the resonance used in the measurement of  $\sigma(\tau)$ . Frequency fluctuations  $\delta\nu$  lead to fluctuations  $\delta N$  in the detected number of atoms.

avoidable magnetic field fluctuations. A state pair with equal magnetic moments such as  $\{|0\rangle, |1\rangle\}$  is therefore much better suited than any other combination of ground state sublevels. In [4], a phase gate with atoms in a magnetic microtrap was proposed, and a gate operation time of 0.4 ms was estimated. By implementing the quantum gate with the qubit studied here,  $\sim 10^3$  gate operations could be performed before decoherence from magnetic fluctuations occurs. The gate operation requires potentials which affect the two qubit states differently. However, a combination of static magnetic and electric fields, as considered in [4, 17], does not provide state-selective potentials for our state pair, whose magnetic moments and electrostatic polarizabilities are equal. Instead, we propose to apply tailored microwave near-fields and make use of the AC Zeeman effect (the magnetic analog of the AC Stark effect). In  $^{87}\text{Rb}$ , AC Zeeman potentials derive from magnetic dipole transitions with a frequency near  $\omega_0/2\pi = 6.835$  GHz between the  $F = 1$  and  $F = 2$  hyperfine manifolds of the ground state. The magnetic component of a microwave field of frequency  $\omega_0 + \Delta$  couples the  $|F = 1, m_F\rangle$  to the  $|F = 2, m_F'\rangle$  sublevels and leads to energy shifts that depend on  $m_F$  and  $m_F'$ . In a spatially varying microwave field, this results in a state-dependent potential landscape.

A microwave trap for neutral atoms based on AC Zeeman potentials has been proposed in [9] and experimentally demonstrated in [10]. This trap employs microwave

radiation in the far field of the source. Due to the centimeter wavelength  $\lambda_{\text{mw}}$  of the radiation, field gradients are very weak and structuring the potential on the micrometer scale is impossible. In magnetic microtraps, on the other hand, atoms are trapped at distances  $d \ll \lambda_{\text{mw}}$  from the chip. Thus, the atoms can be manipulated with microwave near fields, generated by microwave currents in on-chip conductors, which may be fed from a stripline [19]. In the near field of the current configuration, the magnetic component of the microwave field has the same position dependence as a static magnetic field created by equivalent stationary currents. In this way, state-dependent AC Zeeman potentials varying on the micrometer scale can be realized. In combination with state-independent static magnetic microtraps, the complex potential geometries required for QIP can be realized on the chip.

To give a specific example, we consider atoms in a static-field trap at  $d = 10 \mu\text{m}$  from an additional chip wire carrying a microwave current of  $20 \text{ mA}_{\text{pp}}$ . The wire is oriented such that the magnetic component of the microwave field at the position of the atoms is polarized parallel to the static magnetic field in the trap. The microwave couples  $|0\rangle \leftrightarrow |F = 2, m_F = -1\rangle$  and  $|F = 1, m_F = 1\rangle \leftrightarrow |1\rangle$  with identical resonant Rabi frequencies  $\Omega_R/2\pi = 2.4$  MHz. The Zeeman splitting due to the static field (a few MHz) prevents two-photon transitions to other sublevels driven by polarization impurities. For  $\Delta/2\pi = 50$  MHz,  $\Omega_R \ll \Delta$  and the coupling changes the static magnetic moment of the qubit states only by  $\sim 10^{-4} \mu_B$  such that both states still experience the same static-field potentials. The microwave, on the other hand, leads to a differential energy shift of  $|0\rangle$  and  $|1\rangle$ ,  $U_{\text{mw}} \simeq \hbar\Omega_R^2/2\Delta = h \cdot 58$  kHz, sufficiently large for the state-selective manipulation needed in QIP. Besides this application, AC Zeeman potentials can be used to create microtraps for atoms in hyperfine sublevels such as  $m_F = 0$ , which cannot be trapped in a static magnetic trap.

In conclusion, we have performed coherent internal state manipulation in a magnetic microtrap with coherence lifetimes exceeding 1 s at distances down to  $4 \mu\text{m}$  from the chip surface. This paves the way for a variety of applications, most notably chip-based quantum gates and atomic clocks.

We thank T. Udem and M. Zimmermann for providing us with the crystal reference oscillator. Work supported in part by the European Community's IST program under contract ACQP (IST-2001-38863).

\* E-mail: philipp.treutlein@physik.uni-muenchen.de

† Present address: Varian Physics 220, Stanford University, Stanford, CA 94305, U.S.A.

- [1] See, for instance, J. Reichel, *Appl. Phys. B* **75**, 469 (2002), R. Folman *et al.*, *Adv. At. Mol. Opt. Phys.* **48**, 263 (2002), and references therein.
- [2] H. Ott *et al.*, *Phys. Rev. Lett.* **87**, 230401 (2001).
- [3] W. Hänsel *et al.*, *Nature* **413**, 498 (2001).
- [4] T. Calarco *et al.*, *Phys. Rev. A* **61**, 022304 (2000).
- [5] E. Jané *et al.*, *Quant. Inf. Comp.* **3**, 15 (2003).
- [6] W. Hänsel *et al.*, *Phys. Rev. A* **64**, 063607 (2001).
- [7] C. Henkel *et al.*, *Appl. Phys. B* **69**, 379 (1999).
- [8] D.M. Harber *et al.*, *Phys. Rev. A* **66**, 053616 (2002).
- [9] C.C. Agosta *et al.*, *Phys. Rev. Lett.* **62**, 2361 (1989).
- [10] R.J.C. Spreeuw *et al.*, *Phys. Rev. Lett.* **72**, 3162 (1994).
- [11] J. Reichel *et al.*, *Phys. Rev. Lett.* **83**, 3398 (1999).
- [12] N.F. Ramsey, *Molecular Beams* (Clarendon Press, Oxford, 1956).
- [13] S. Schneider *et al.*, *Phys. Rev. A* **67**, 023612 (2003).
- [14] M.P.A. Jones *et al.*, *Phys. Rev. Lett.* **91**, 080401 (2003).
- [15] D.M. Harber *et al.*, *J. Low Temp. Phys.* **133**, 229 (2003).
- [16] Y. Lin *et al.*, cond-mat/0308457 (2003).
- [17] P. Krüger *et al.*, quant-ph/0306111 (2003).
- [18] See, for instance, G. Santarelli *et al.*, *Phys. Rev. Lett.* **82**, 4619 (1999).
- [19] T.C. Edwards, *Foundations for microstrip circuit design* (John Wiley & Sons, Chichester, 1981)